

## A stable surface construction of Ni-rich $\text{LiNi}_{0.8}\text{Mn}_{0.1}\text{Co}_{0.1}\text{O}_2$ cathode material for high performance lithium-ion batteries

*Yu Li,<sup>a,c</sup> Chunlei Tan,<sup>a,c</sup> Shaomei Wei,<sup>a</sup> Lisan Cui,<sup>a,c</sup> Xiaoping Fan,<sup>a,c</sup> Qichang*

*Pan,<sup>\*,a,c</sup> Feiyan Lai,<sup>b</sup> Fenghua Zheng,<sup>\*,a,c</sup> Hongqiang Wang,<sup>a,c</sup> Qingyu Li,<sup>a,c</sup>*

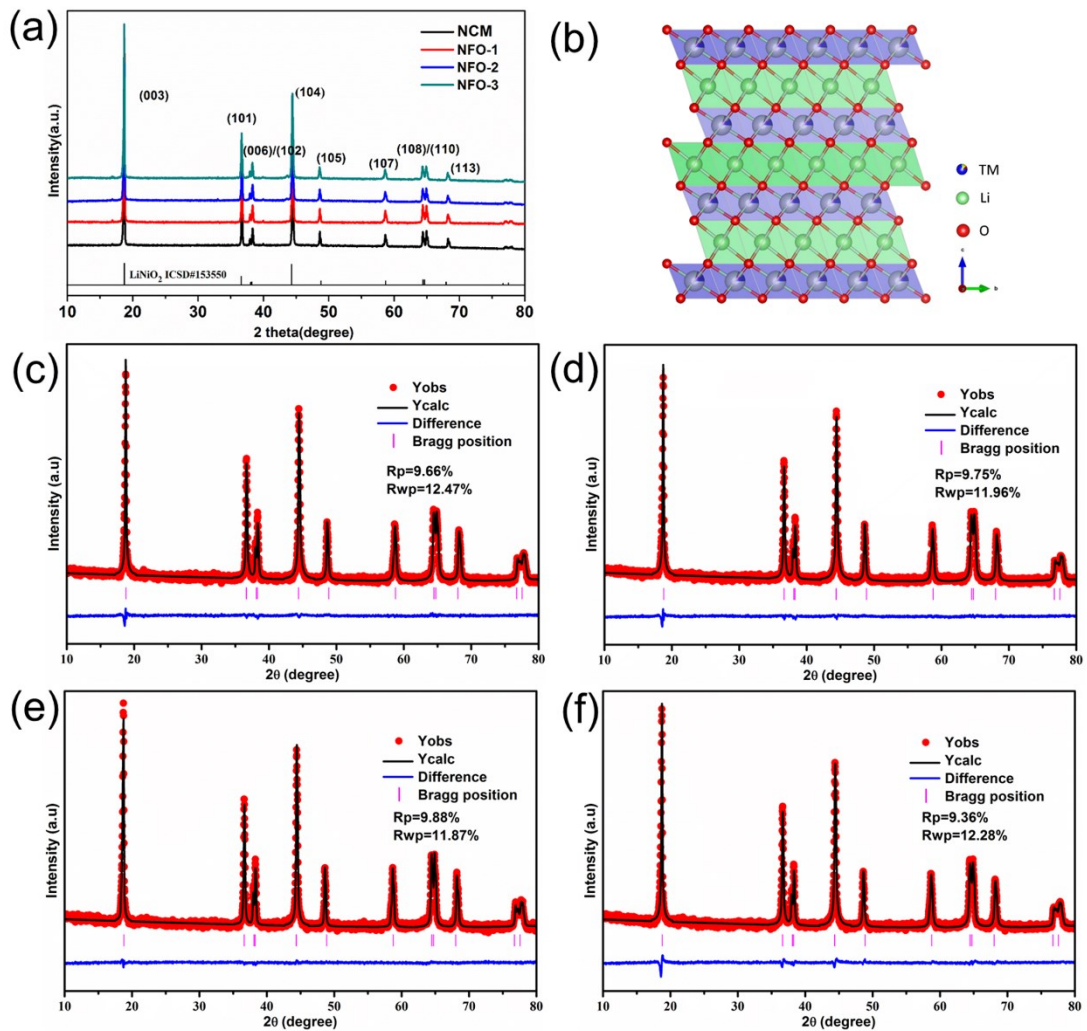
<sup>a</sup> Guangxi Key Laboratory of Low Carbon Energy Materials, School of Chemistry and Pharmaceutical Sciences, Guangxi Normal University, Guilin 541004, China.

<sup>b</sup> Guangxi Key Laboratory of Comprehensive Utilization of Calcium Carbonate Resources, College of Materials and Environmental Engineering, Hezhou University, Hezhou 542899, China.

<sup>c</sup> Guangxi New Energy Ship Battery Engineering Technology Research Center, Guangxi Normal University, Guilin, 541004, China.

\* Corresponding author.

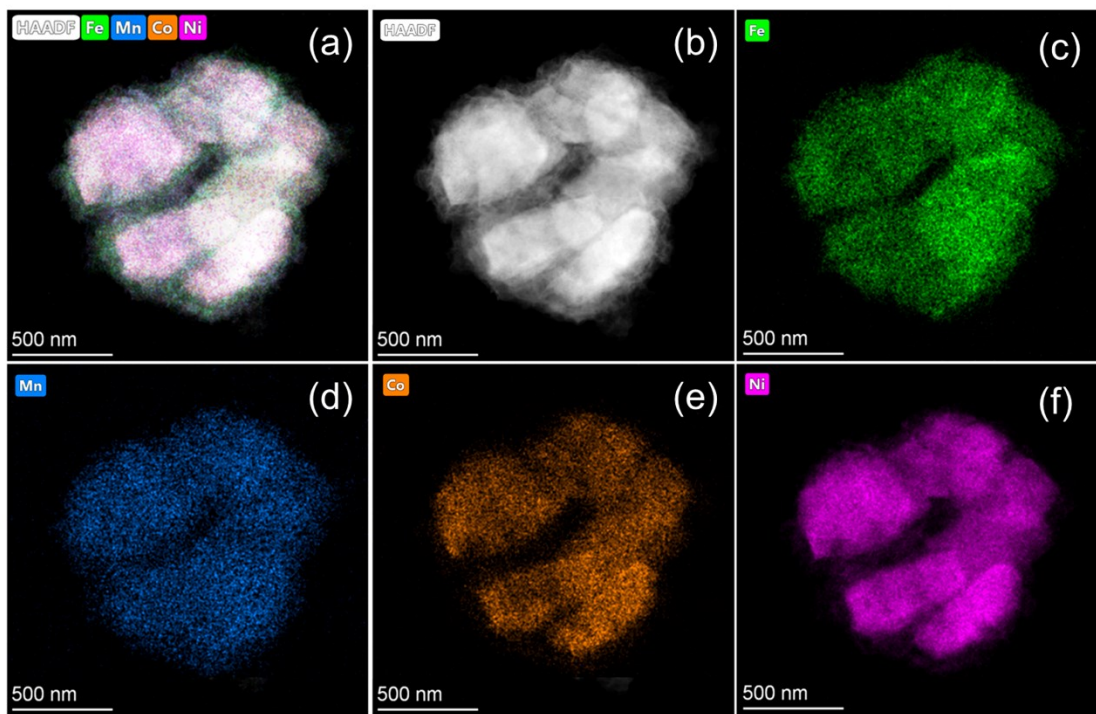
E-mail: panqc0526@163.com (Q. Pan); zhengfh870627@163.com (F. Zheng).



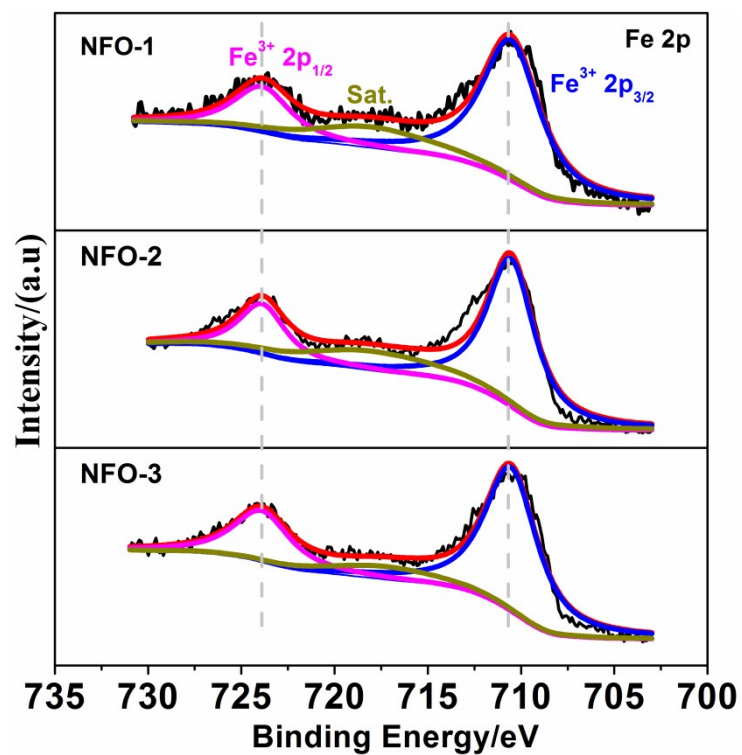
**Figure S1.** (a) XRD patterns of NCM and all modified samples; (b) The crystal structure diagram of NCM; Rietveld refinement plot of (c) NCM, (d) NFO-1, (e) NFO-2 and (f) NFO-3, respectively.

**Table S1.** Crystal structural parameters of NCM, NFO-1, NFO-2 and NFO-3, respectively.

Samples	a(Å)	c(Å)	volume(Å <sup>3</sup> )	c/a	Rp(%)	Rwp(%)
NCM	2.8717	14.1997	101.4156	4.9447	9.66	12.47
NFO-1	2.8724	14.2011	101.4696	4.9440	9.75	11.96
NFO-2	2.8742	14.2024	101.6056	4.9413	9.88	11.87
NFO-3	2.8736	14.1973	101.5306	4.9405	9.36	12.28



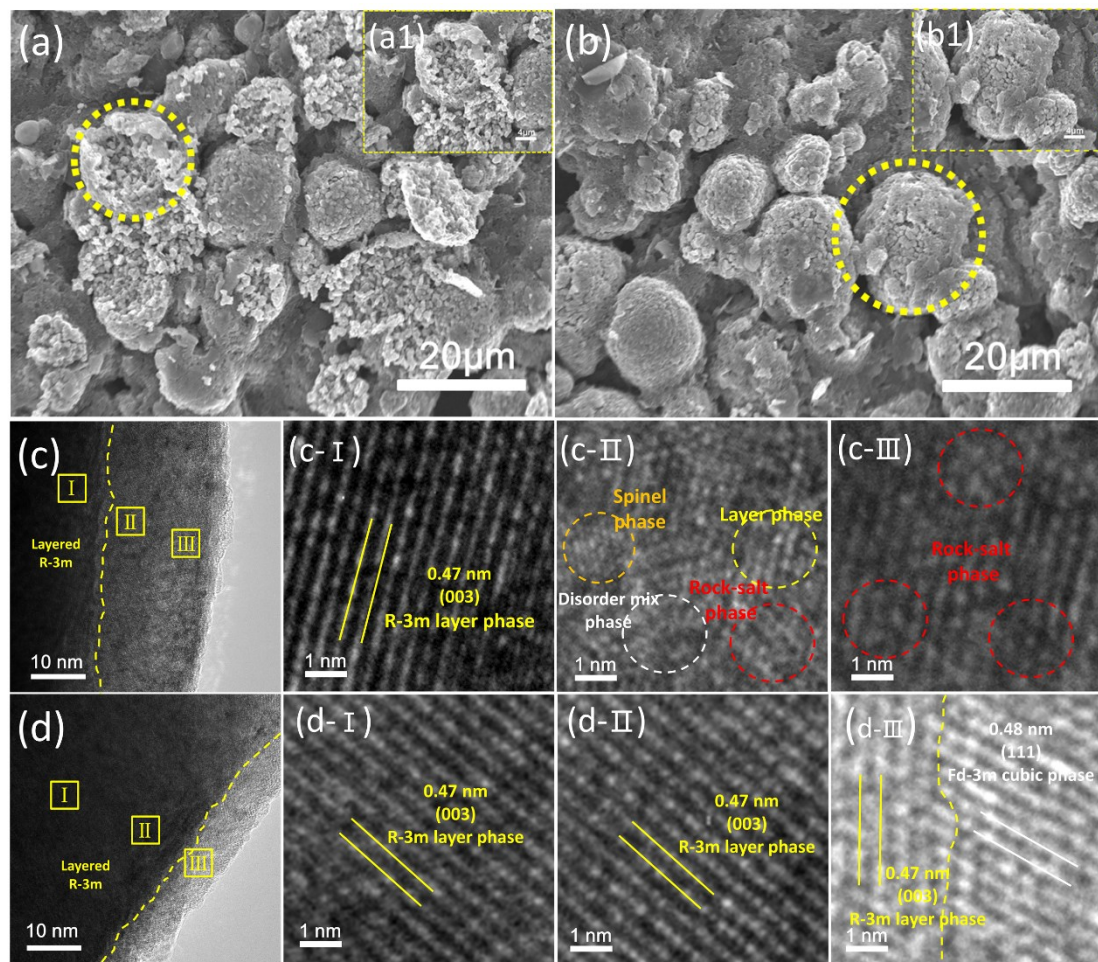
**Figure S2.** STEM-EDS mapping results for NFO-2 samples, corresponding to the detected elements (c) Fe, (d) Mn, (e) Co, and (f) Ni elements.



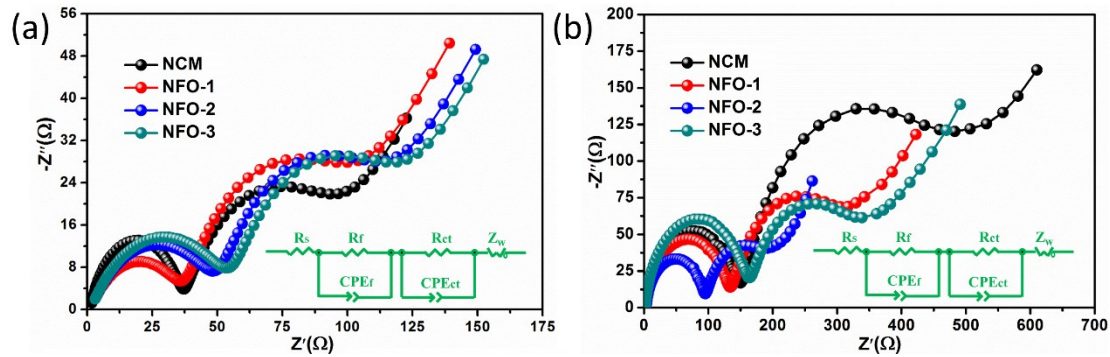
**Figure S3.** XPS spectra of Fe 2p of NFO-1, NFO-2 and NFO-3, respectively.

Table S2 PH value and residual lithium content of NCM, NFO-1, NFO-2 and NFO-3, respectively.

Samples	PH	Residual lithium (ppm)
NCM	11.48	2176.3
NFO-1	11.35	1588.9
NFO-2	11.26	1476.2
NFO-3	11.21	1395.2



**Figure S4.** The SEM and HR-TEM of (a, c) NCM and (b, d) NFO-2 after 250 cycles.



**Figure S5.** Impedance spectra of NCM and modified samples at 4.4 V during the charging process after (a) 1st and (b) 250th cycles. The insert shows the corresponding equivalent circuit of the fitting.

**Table S3.** EIS fitting data of NCM and all  $\text{NiFe}_2\text{O}_4$  modified samples.

samples	Initial cycle		After 250 cycles	
	Interfacial Resistance			
	$R_f/\Omega$	$R_{ct}/\Omega$	$R_f/\Omega$	$R_{ct}/\Omega$
NCM	36.3	53.9	342.2	141
NFO-1	36.4	54	184	127.7
NFO-2	51.9	49.7	94.1	89.0
NFO-3	54.7	51.1	152.9	198.6

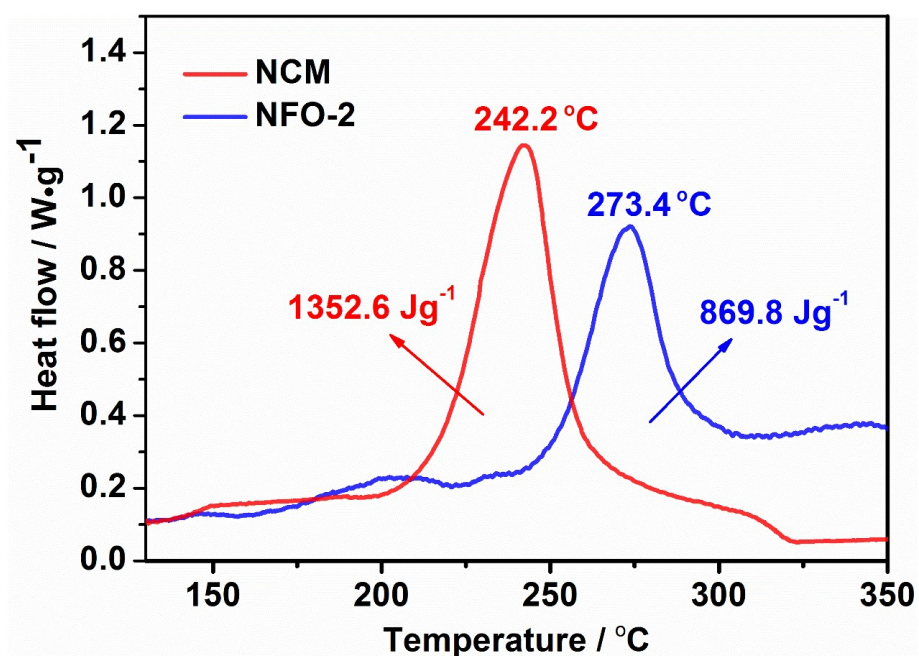


**Figure S6.** DSC profiles of NCM and NFO-2 cathodes at charged state to 4.4 V.

Table S4. The electronic conductivity of NCM and NFO coating samples.

Samples	Electrical conductivity (S/cm <sup>-1</sup> )
NCM	$2.04 \times 10^{-4}$
NFO-1	$2.56 \times 10^{-4}$
NFO-3	$3.43 \times 10^{-4}$
NFO-3	$1.95 \times 10^{-4}$

**Table S5.** The electrochemical properties of our work and other literatures about NCMs.

Rate properties / mAh•g <sup>-1</sup>		Capacity retention rate / %		References
5C	10C	100th	200th	
161.1	/	/	81.2	S1
177.1	/	90	/	S2
120.5	/	/	80.38	S3
161.5	125.0	88	/	S4
148.0	135.2	/	85.8	S5
165.0	143.5	91.6	/	S6
158.5	137.06	/	89.43	S7
147.5	107.1	87.3%	/	S8
131.02	/	76.07%	/	S9
177.3	140.56	97.8	90.75	Our work

### References

- S1 K. Yuan, N. Li, R. Ning, C. Shen, N. Hu, M. Bai, K. Zhang, Z. Tian, L. Shao, Z. Hu, X. Xu, T. Yu and K. Xie, Nano Energy, 2020, 78, 105239.
- S2 Y. Liu, L.-b. Tang, H.-x. Wei, X.-h. Zhang, Z.-j. He, Y.-j. Li and J.-c. Zheng, Nano Energy, 2019, 65, 104043.
- S3 H. Liang, S. Yuan, L. Shi, Y. Zhao, Z. Wang and J. Zhu, Chemical Engineering Journal, 2020, 394, 124846.
- S4 J. Hwang, K. Do and H. Ahn, Chemical Engineering Journal, 2020, 126813.
- S5 W. Tang, Z. Chen, F. Xiong, F. Chen, C. Huang, Q. Gao, T. Wang, Z. Yang and W. Zhang, J. Power Sources, 2019, 412, 246-254.

- S6 X. Qi, Z. Xue, K. Du, Y. Xie, Y. Cao, W. Li, Z. Peng and G. Hu, *J. Power Sources*, 2018, 397, 288-295.
- S7 W. Yang, W. Xiang, Y.-X. Chen, Z.-G. Wu, W.-B. Hua, L. Qiu, F.-R. He, J. Zhang, B.-H. Zhong and X.-D. Guo, *ACS Appl. Mater. Interfaces*, 2020, 12, 10240-10251.
- S8 R. Qian, Y. Liu, T. Cheng, P. Li, R. Chen, Y. Lyu and B. Guo, *ACS Appl. Mater. Interfaces*, 2020, 12, 13813-13823.
- S9 Y. Zhang, T. Ren, J. Zhang, J. Duan, X. Li, Z. Zhou, P. Dong and D. Wang, *Journal of Alloys and Compounds*, 2019, 805, 1288-1296.

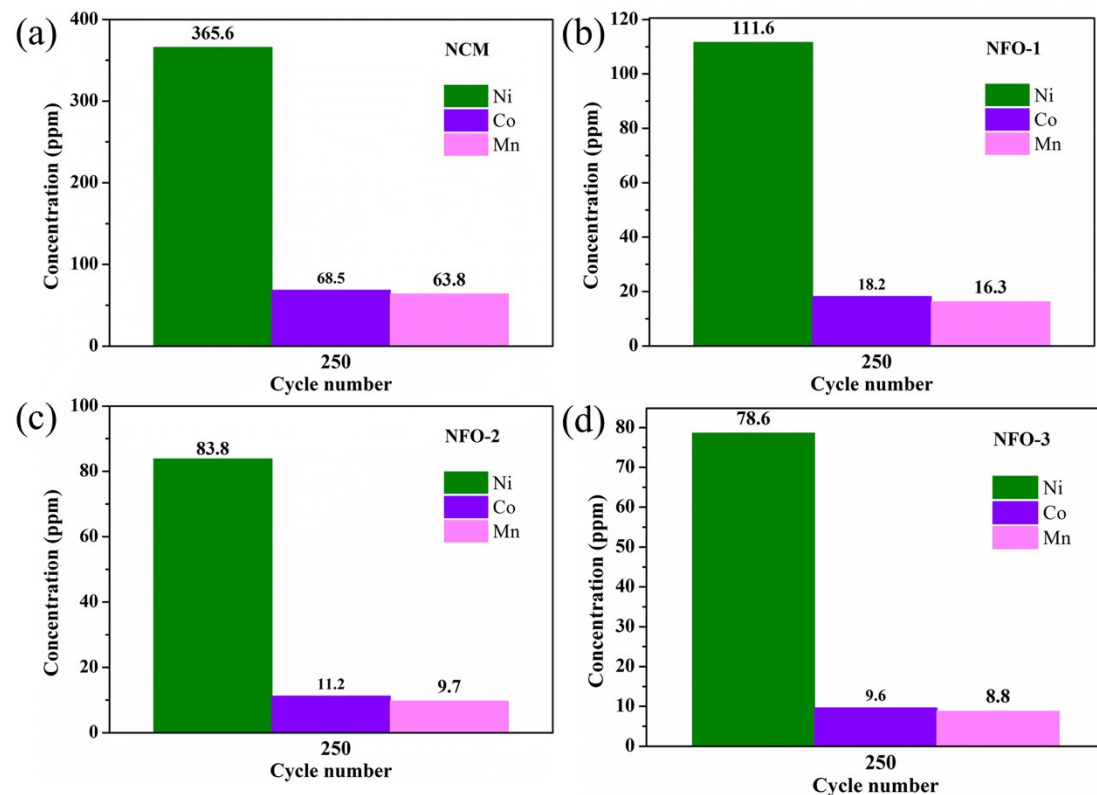


Figure S7. The ICP-OES quantification results for dissolved transition metal

component after 250 cycles of (a) NCM and (b-d) NFO-coated samples.